ORGANIC LETTERS

2008
Vol. 10, No. 12
2513−2516

Supramolecular Multicomponent Self-Assembly of Shape-Adaptive Nanoprisms: Wrapping up C_{60} with Three Porphyrin Units

Michael Schmittel,* Bice He, and Prasenjit Mal

Center for Micro- and Nanochemistry and Engineering, Organische Chemie I, Universität Siegen, D-57068 Siegen, Germany

schmittel@chemie.uni-siegen.de

Received April 7, 2008

ABSTRACT

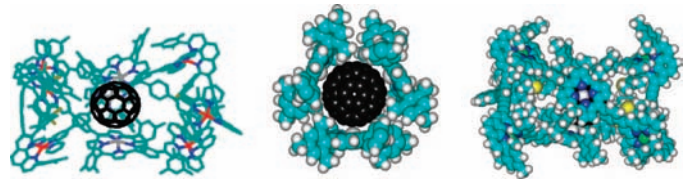

Self-assembly of a C_{3v} symmetric trisphenanthroline and linear bisterpyridines in the presence of Cu^{+} did not furnish the expected supramolecular nanoprisms in quantitative yield. With an accurately sized tripyridine as a stabilizing template, the nanoprism formed exclusively. Furthermore, an adaptive constriction of the nanoprism was seen with C_{60} as template: as a result of the smaller size of C_{60} the nanoframework wrapped up around the guest like an accordion-type host system.

Self-assembly, a burgeoning section of supramolecular chemistry, has been a prolific tool for the construction of diverse fascinating hollow 3D structures, such as Fujita's cages[1] and hexahedra;[2] Atwood's snub cube;[3] Stang's prism,[4] cuboctahedra,[5] and dodecahedra;[6] Raymond's tetrahedra;[7] etc. These structures are spectacular not only because of their size and shape but also because of their ability to encapsulate neutral[7] or charged guest[8] molecules via noncovalent interactions. Yet, almost all known host−guest complexes formed from nanosized, self-assembled aggregates are rather static, indicating that our ability to set up systems for adaptive shape transformations is still limited.[9] Herein, we disclose how an added guest decisively modulates the shape of a supramolecular three-component assembly affording either a nanoprism through templation or a constricted nanoframework wrapped up around a C_{60} unit.

In contrast to Süss-Fink and Therrien,[10] Hupp,[11] and Su,[12] we focused on a *three-component* self-assembly protocol toward nanoprisms utilizing the HETTAP (Heteroleptic Terpyridine And Phenanthroline Metal Complexes) concept.

(1) (a) Fujita, M.; Oguro, D.; Miyazawa, M.; Oka, H.; Yamaguchi, K.; Ogura, K. *Nature* **1995**, *378*, 469–471. (b) Kumazawa, K.; Biradha, K.; Kusukawa, T.; Okano, T.; Fujita, M. *Angew. Chem., Int. Ed.* **2003**, *42*, 3909–3913.

(2) Takeda, N.; Umemoto, K.; Yamaguchi, K.; Fujita, M. *Nature* **1999**, *398*, 794–796.

(3) MacGillivray, L. R.; Atwood, J. L. *Nature* **1997**, *389*, 469–472.

(4) Kuehl, C. J.; Yamamoto, T.; Seidel, S. R.; Stang, P. J. *Org. Lett.* **2002**, *4*, 913–915.

(5) Olenyuk, B.; Whiteford, J. A.; Fechtenkötter, A.; Stang, P. J. *Nature* **1999**, *398*, 796–799.

(6) Olenyuk, B.; Levin, M. D.; Whiteford, J. A.; Shield, J. E.; Stang, P. J. *J. Am. Chem. Soc.* **1999**, *121*, 10434–10435.

(7) Biros, S. M.; Bergman, R. G.; Raymond, K. N. *J. Am. Chem. Soc.* **2007**, *129*, 12094–12095.

(8) Fiedler, D.; Leung, D. H.; Bergman, R. G.; Raymond, K. N. *J. Am. Chem. Soc.* **2004**, *126*, 3674–3675.

(9) Lehn, J.-M. *Chem. Soc. Rev.* **2007**, *36*, 151–160.

(10) (a) Govindaswamy, P.; Linder, D.; Lacour, J.; Süss-Fink, G.; Therrien, B. *Chem. Commun.* **2006**, 4691–4693. (b) Govindaswamy, P.; Süss-Fink, G.; Therrien, B. *Organometallics* **2007**, *26*, 915–924.

(11) Lee, S. J.; Mulfort, K. L.; O'Donnell, J. L.; Zuo, X.; Goshe, A. J.; Wesson, P. J.; Nguyen, S. T.; Hupp, J. T.; Tiede, D. M. *Chem. Commun.* **2006**, 4581–4583.

(12) Liu, Z.-M.; Liu, Y.; Zheng, S.-R.; Yu, Z.-Q.; Pan, M.; Su, C.-Y. *Inorg. Chem.* **2007**, *46*, 5814–5816.

10.1021/ol800796h CCC: $40.75
Published on Web 05/27/2008

This strategy (Figure 1) exploits steric and electronic effects originating from bulky aryl substituents at the phenanthroline

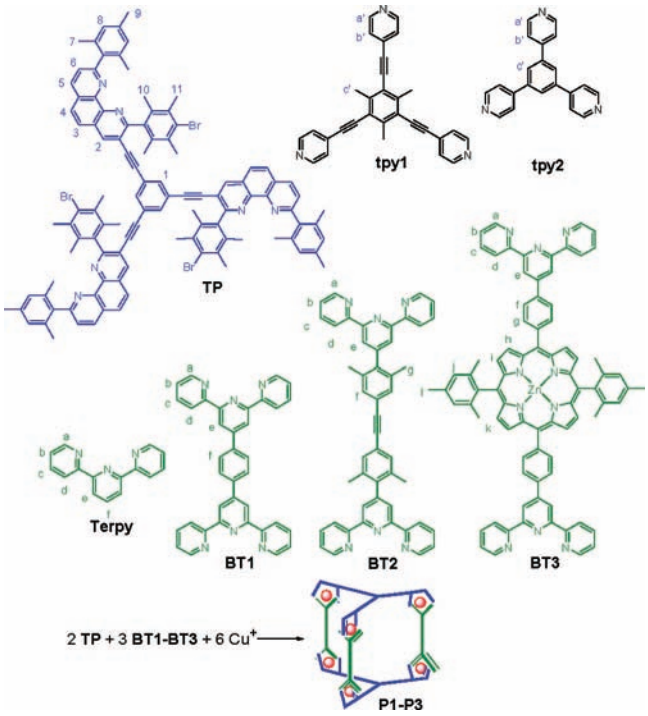

Figure 1. Ligands, such as trisphenanthroline, tripyridines, and terpyridines, used in the self-assembly of nanoprisms **P1**−**P3**.

to control the coordination equilibrium at the metal ion.[13] Use of Cu^{+} should be optimal for generating mixed [M(phen)-(terpy)]$^{n+}$ complexes, as it avoids having too strong a driving force for bishomoleptic [M(terpy)$_2$]$^{n+}$ complexes, quite in contrast to Zn^{2+}.[14]

Trisphenanthroline **TP** (see Figure 1) was synthesized by a Sonogashira cross-coupling of 1,3,5-triiodobenzene[15] and the terminal alkynylphenanthroline, the latter prepared by a procedure described earlier.[16] Bisterpyridine **BT1** was purchased, while **BT2** was prepared as reported.[13c] Bisterpyridine **BT3** was synthesized by a Suzuki cross-coupling of [2,2′:6′,2″]-terpyridinyl-4′-boronic acid and zinc(II)-5,15-bis(4-bromophenyl)-10,20-dimesitylporphyrin (see Supporting Information).

To slow down formation of the undesired [Cu(terpy)$_2$]$^{+}$ complexes, [Cu(MeCN)$_4$]PF$_6$ and **TP** were first reacted with each other in dichloromethane for 5 min, and then solutions of **BT1**, **BT2** (in dichloromethane), and **BT3** (in chloroform) were added to form the heteroleptic nanoprisms **P1**−**P3**. From solutions of **P1** = [Cu$_6$(**TP**)$_2$(**BT1**)$_3$]$^{6+}$ and **P2** = [Cu$_6$(**TP**)$_2$(**BT2**)$_3$]$^{6+}$ in dichloromethane, ESI-MS signals of notable intensity were observed arising from the 4+, 5+, and 6+ charged prisms, while their ^{1}H NMR spectra (see Figure 2) were characterized by atypically broad absorptions.

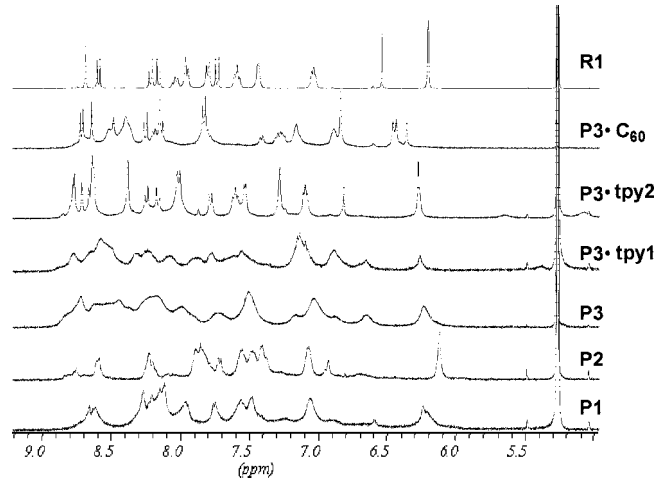

Figure 2. Partial ^{1}H NMR spectra of complexes **R1**, **P1**−**P3**, and **P3**·template with **P1** = [Cu$_6$(**TP**)$_2$(**BT1**)$_3$]$^{6+}$, **P2** = [Cu$_6$(**TP**)$_2$(**BT2**)$_3$]$^{6+}$, **P3** = [Cu$_6$(**TP**)$_2$(**BT3**)$_3$]$^{6+}$, and **R1** = [Cu$_3$(**TP**)(**Terpy**)$_3$]$^{3+}$.

Solutions of **P1** and **P2** in acetonitrile, after being heated to various temperatures between room temperature and 79 °C, furnished identical spectra at room temperature, precluding kinetic control in the assembly process. For **P1** and **P2** signals sharpened notably at −30 °C but still represented more than one species, thus suggesting the occurrence of other thermodynamically competitive species in the mixture. When we used the longest bisterypridine, **BT3**, in the self-assembly, the alleged **P3** = [Cu$_6$(**TP**)$_2$(**BT3**)$_3$]$^{6+}$ was formed in even smaller amounts, as noted from both ESI-MS and ^{1}H NMR data. However, the signal at ca. 6.2 ppm in all spectra of **P1**−**P3** clearly pointed to the compelling formation of the desired heteroleptic copper(I) complexes.

In contrast, the simple complex [Cu$_3$(**TP**)(**Terpy**)$_3$]$^{3+}$ = **R1** was formed in a clean manner after mixing [Cu(MeCN)$_4$]PF$_6$, **TP**, and the parent terpyridine (**Terpy**) as evidenced by the clean ESI-MS signal set and sharp resonances in the ^{1}H NMR spectrum. After comparing these results with those of the prisms, we reasoned that complete formation of **P1**−**P3** was impeded due to the thermodynamically competitive formation of some small oligomeric aggregates.

(13) Steric stoppers at the phenanthroline's coordination site in 2,9-position prevent any competitive bishomoleptic metal phenanthroline complexes, therefore leading preferably to hetero combinations: (a) Schmittel, M.; Kalsani, V.; Fenske, D.; Wiegrefe, A. *Chem. Commun.* **2004**, 490–491. (b) Schmittel, M.; Kalsani, V.; Kishore, R. S. K.; Cölfen, H.; Bats, J. W. *J. Am. Chem. Soc.* **2005**, *127*, 11544–11545. (c) Schmittel, M.; Kalsani, V.; Mal, P.; Bats, J. W. *Inorg. Chem.* **2006**, *45*, 6370–6377. (d) Schmittel, M.; He, B.; Kalsani, V.; Bats, J. W. *Org. Biomol. Chem.* **2007**, *5*, 2395–2403.

(14) Schmittel, M.; Mal, P. *Chem. Commun.* **2008**, 960–962.

(15) Vatsadze, S. Z.; Titanyuk, I. D.; Chernikov, A. V.; Zyk, N. V. *Russ. Chem. Bull., Int. Ed.* **2004**, *53*, 471–473.

(16) (a) Schmittel, M.; Michel, C.; Wiegrefe, A.; Kalsani, V. *Synthesis* **2001**, 1561–1567. (b) Schmittel, M.; Michel, C.; Wiegrefe, A. *Synthesis* **2005**, 367–373.

(17) (a) Anderson, H. L.; Walter, C. J.; Vidal-Ferran, A.; Hay, R. A.; Lowden, P. A.; Sanders, J. K. M. *J. Chem. Soc., Perkin Trans. 1* **1995**, 2275–2279. (b) Anderson, S.; Anderson, H. L.; Bashall, A.; McPartlin, M.; Sanders, J. K. M. *Angew. Chem., Int. Ed.* **1995**, *34*, 1096–1099.

Since zinc porphyrin can form strong complexes with pyridines[11,17] and fullerenes,[18] we chose the tripyridines **tpy1**[19] and **tpy2** as well as C_{60} as templates to stabilize the prism **P3**. Not unexpectedly, all attempts to fit the large **tpy1** (requesting $d_{Zn-Zn} = 1.78$ nm in a trigonal arrangement of three zinc porphyrins, see Figure 3) into prism **P3** (providing

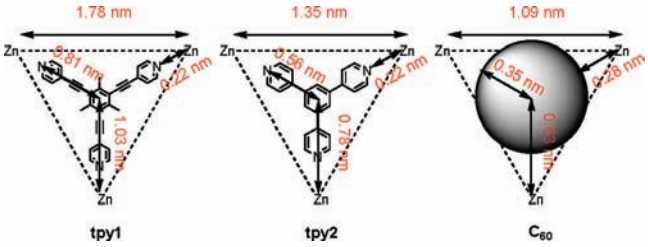

Figure 3. Zn−Zn distances in an idealized, prism-like trigonal setting of three zinc porphyrins complexing to **tpy1**, **tpy2**, and fullerene C_{60} (from MM^+ minimized molecular models; a typical $Zn_{Por}-N_{Py}$ coordination distance of 0.22 nm was assumed[17b]).

$d_{Zn-Zn} = 1.45$ nm) failed to afford **P4** = **P3**·**tpy1** in good yield as judged by ESI-MS and NMR.

In contrast, **tpy2**, requiring a d_{Zn-Zn} of 1.35 nm, is a highly suitable template for **P3** since its size closely matched that of **P3** as shown in Figure 4. After addition of **tpy2** to **P3**, the ESI-MS spectrum (see Supporting Information) exhibited two main signals at 1284.3 and 1570.5 Da representing the 6+ and 5+ charged prism **P5** = **P3**·**tpy2**, i.e., $[Cu_6(\mathbf{TP})_2(\mathbf{BT3})_3(\mathbf{tpy2})]^{6+}$ and $[Cu_6(\mathbf{TP})_2(\mathbf{BT3})_3(\mathbf{tpy2})(PF_6)]^{5+}$, respectively. Absence of peaks at 1233.4, 1509.1, and 1922.7 Da for the 6+, 5+, and 4+ charged prism **P3** suggested exclusive formation of **P5**. The ^{1}H NMR analysis of **P5** in CD_2Cl_2/CD_3CN (4:1) revealed only one set of signals with the chemical shift of the 8-H mesityl proton of **TP** being diagnostically shifted from 6.96 to 6.33 ppm (see Figure 2). Additionally, the chemical shifts of the **tpy2** pyridine protons, initially located at 8.59 and 7.59 ppm in $CDCl_3$, were dramatically shifted to 5.71 and 5.13 ppm. Existence of **P5** as a single species was conclusively established by DOSY ^{1}H NMR (see Supporting Information). Hence, one has to conclude that the strong binding and good spatial match between the three pyridine nitrogens of **tpy2** and the three zinc porphyrin units in **P3** transfers a dynamic mixture into a single species **P5**.

(18) (a) Tashiro, K.; Aida, T.; Zheng, J.-Y.; Kinbara, K.; Saigo, K.; Sakamoto, S.; Yamaguchi, K. *J. Am. Chem. Soc.* **1999**, *121*, 9477–9478. (b) Zheng, J.-Y.; Tashiro, K.; Hirabayashi, Y.; Kinbara, K.; Saigo, K.; Aida, T.; Sakamoto, S.; Yamaguchi, K. *Angew. Chem., Int. Ed.* **2001**, *40*, 1858–1861. (c) Wang, Y.-B.; Lin, Z. *J. Am. Chem. Soc.* **2003**, *125*, 6072–6073. (d) Boyd, P. D. W.; Reed, C. A. *Acc. Chem. Res.* **2005**, *38*, 235–242. (e) Satake, A.; Kobuke, Y. *Tetrahedron* **2005**, *61*, 13–41. (f) Hosseini, A.; Taylor, S.; Accorsi, G.; Armaroli, N.; Reed, C. A.; Boyd, P. D. W. *J. Am. Chem. Soc.* **2006**, *128*, 15903–15913. (g) Ouchi, A.; Tashiro, K.; Yamaguchi, K.; Tsuchiya, T.; Akasaka, T.; Aida, T. *Angew. Chem., Int. Ed.* **2006**, *45*, 3542–3546. (h) Olmstead, M. M.; Nurco, D. J. *Cryst. Growth Des.* **2006**, *6*, 109–113. (i) Hosseini, A.; Hodgson, M. C.; Tham, F. S.; Reed, C. A.; Boyd, P. D. W. *Cryst. Growth Des.* **2006**, *6*, 397–403.

(19) Asselberghs, I.; Hennrich, G.; Clays, K. *J. Phys. Chem. A* **2006**, *110*, 6271–6275.

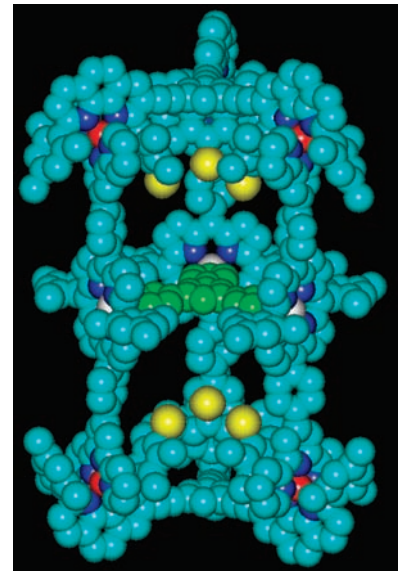

Figure 4. Side view of space-filling presentation of prism **P5** = **P3**·**tpy2** as generated from force field modeling (Hyperchem). The atoms/ligand are color coded for clarity: carbon, cyan; nitrogen, blue; bromine, yellow; copper, red; zinc, white; **tpy2** ligand, green. Hydrogens are removed for clarity.

Notably, the smaller C_{60} requiring a Zn−Zn distance of only 1.09 nm for complexation (see Figure 3) also proved to be a good template for **P3**. Due to the low solubility of C_{60} in acetonitrile, C_{60} (1 equiv per **P3**) was added in carbon disulfide to an acetonitrile solution of **P3**. After removal of all solvents, the solid residue, now **P6** = **P3**·C_{60}, was dissolved in CD_3CN and analyzed by ESI-MS, ^{1}H NMR, ^{13}C NMR, UV−vis, CV, and DPV without further purification. The ^{1}H NMR spectrum of **P6** was significantly simplified compared to that of **P3** (Figure 2). Its ^{13}C NMR spectrum showed a strong signal at $\delta = 139.4$ ppm, unmistakably indicating the presence of bound C_{60}, as free C_{60}, studied in a control experiment, exhibited a signal shifted downfield by $\Delta\delta \sim 4$ ppm.[20] The ESI-MS (Supporting Information) displayed two main signals at 1652.0 and 1352.8 Da from the 5+ and 6+ charged **P6**, i.e., $[Cu_6(\mathbf{TP})_2(\mathbf{BT3})_3(C_{60})\ (PF_6)]^{5+}$ and $[Cu_6(\mathbf{TP})_2\ (\mathbf{BT3})_3(C_{60})]^{6+}$, respectively. Also their isotopic splitting was in good agreement with those from simulations. If harsher ionization conditions were applied (offset increased, higher temperature), two extra signals at 1233.5 Da for $[Cu_6(\mathbf{TP})_2(\mathbf{BT3})_3]^{6+}$ and at 1511.5 Da for $[Cu_6(\mathbf{TP})_2(\mathbf{BT3})_3(PF_6)]^{5+}$ were observed, suggesting that **P6** can release C_{60}. It is noteworthy that the porphyrin−fullerene interaction has rarely been documented by ESI-MS analysis,[18a,f] hence suggesting an unusually strong binding between **P3** and C_{60} in **P6**.

Cyclic (CV) and differential pulse voltammograms (DPV) further confirmed that C_{60} was entrapped in **P6**. Due to

(20) As C_{60} has a very low solubility of 8 μg mL^{-1} in acetonitrile (Marcus, Y.; Smith, A. L.; Korobov, M. V.; Mirakyan, A. L.; Avramenko, N. V.; Stukalin, E. B. *J. Phys. Chem. B* **2001**, *105*, 2499–2506.) we measured its ^{13}C signal in a 1:1 mixture of toluene/acetonitrile. See Supporting Information, Figures S31 and S32.

solubility problems in presence of the electrolyte, CV and DPV measurements of **P3** and **P6** were conducted in THF/acetonitrile (1:1) using tetra-*n*-butyl-ammonium hexafluorophosphate as electrolyte. The CV and DPV spectra showed two waves corresponding to the reduction $C_{60}^{0/-}$ and $C_{60}^{-/2-}$ at −0.94 and −1.38 V vs ferrocene (Fc) confirming the presence of C_{60} in **P6** (Figure 5, Figure S3). Besides,

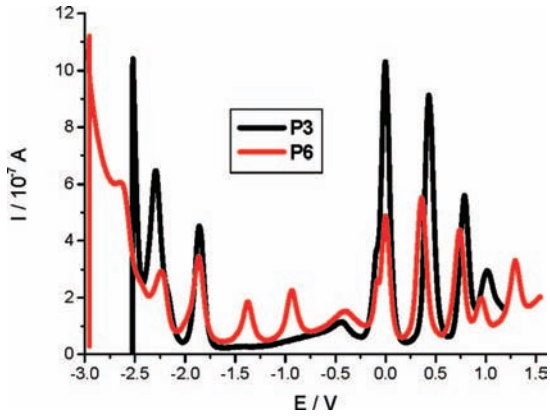

Figure 5. DPV of **P3** (black) and **P6** = **P3**·C_{60} (red) measured in acetonitrile/THF (1:1) using ferrocene as internal standard.

the oxidation potential of $Cu^{+/2+}$ was shifted from 0.43 to 0.36 V, the $ZnP^{0/+}$ wave was shifted from 0.79 to 0.74 V, and that of $ZnP^{+/2+}$ was shifted from 1.02 to 0.96 V. These small cathodic shifts of about 60 mV exhibited by the zinc porphyrin units in **P6** are obviously due to their interaction with C_{60}.

The sum of evidence indicates that C_{60} is strongly bound inside the prism **P6** = **P3**·C_{60}: (i) a templating role of C_{60} can only become effective inside **P3**, and (ii) ESI-MS, CV, and DPV advocate strong interactions between **P3** and C_{60}. However, in order to make use of three porphyrin units,[18g–i] **P6** needs to have a constricted geometry properly adapting to the size of the encapsulated fullerene. A model study (MM^+ in Hyperchem) suggests that this is easily possible by twisting the C_{3v} top versus the C_{3v} bottom deck (see Graphical Abstract and Supporting Information). This adaptive distortion of the host is well evinced in the NMR! A detailed comparison of the ^{1}H NMRs (Figure 2) indicates there are several atypical proton shifts and splittings in **P6** that are not there in **P3**, **P5**, **R1**, **TP**, and **BT3**: (i) Protons 1-H of **TP** are shifted highfield in **P6** by about 0.2−0.4 ppm as compared to those in **R1** and **P5**. (ii) Protons 8-H of the phenanthroline unit seen at identical δ 6.3 ppm in **P3**, **P5**, and **R1** are shifted 0.3 ppm downfield and split into two singlets with an integration ratio of 1:1 for **P6**. Whereas the high field shift in **P3**, **P5**, and **R1** advocates a positioning of 8-H in the shielding region of the terpyridine ligand due to the complex geometry, the lowfield shift in **P6** in contrast suggests a partial egression from this spatial region. The signal splitting moreover indicates that the phenanthroline is not any more representing a plane of symmetry in **P6**, obviously due to its twisted structure. The sum of data thus strongly supports the adaptive complexation of C_{60} in a constricted inner cavity of **P6**.

In summary, we have demonstrated that nanoprisms can be prepared from multicomponent self-assembly of the trisphenanthroline **TP** and various bisterpyridines **BT1**−**BT3** following the HETTAP strategy. Different from the situation with the analogous but quantitatively formed nanoladder systems investigated earlier,[13] the nanoprisms **P1**−**P3** are formed in equilibrium with smaller oligomers. After adding templates of suitable size, such as **tpy2** or C_{60}, interaction between the latter and the porphyrin unit of **BT3** provided an extra driving force that shifted the equilibrium completely toward the desired structures. Thus, with **tpy2** the prism **P5** = **P3**·**tpy2** was formed. In contrast, with C_{60} as template the nanoprism **P3** acted as an adaptive host leading to the constricted prism **P6** = **P3**·C_{60}. As such, **P3** represents an interesting type of host system changing its longitudinal dimensions in order to adapt laterally to the size of the guest, somewhat similar to an accordion. Clearly, its modus operandi is different from that of longitudinally adaptive hosts.[18a]

Acknowledgment. We are grateful to the Deutsche Forschungsgemeinschaft, the Humboldt Foundation and the Fonds der Chemischen Industrie for financial support.

Supporting Information Available: Experimental procedures and spectroscopic data for all new ligands and nanoprisms. This material is available free of charge via the Internet at http://pubs.acs.org.

OL800796H